https://ntrs.nasa.gov/search.jsp?R=19660005482 2020-03-24T04:17:44+00:00Z

NASA TECHNICAL MEMORANDUM

NASA TM X-52151

NASA TM X-52151

N66-14771

(ACCESSION NUMBER) (THRU)

35 1

(PAGES) (CODE)

33

(NASA CR OR TMX OR AD NUMBER) (CATEGORY)

FACILITY FORM 602

GPO PRICE $

CFSTI PRICE(S) $

Hard copy (HC) 2.00

Microfiche (MF) .50

ff 653 July 65

AN EXPERIMENTAL STUDY OF THE CONDENSING CHARACTERISTICS OF MERCURY VAPOR FLOWING IN SINGLE TUBES

by James A. Albers and David Namkoong, Jr.
Lewis Research Center
Cleveland, Ohio

TECHNICAL PAPER proposed for presentation at
Rankine Cycle Specialists Conference sponsored by the
American Institute of Aeronautics and Astronautics
Cleveland, Ohio, October 26-28, 1965

NATIONAL AERONAUTICS AND SPACE ADMINISTRATION · WASHINGTON, D.C. · 1965

AN EXPERIMENTAL STUDY OF THE CONDENSING CHARACTERISTICS OF MERCURY VAPOR FLOWING IN SINGLE TUBES

by James A. Albers and David Namkoong, Jr.

Lewis Research Center
Cleveland, Ohio

TECHNICAL PAPER proposed for presentation at

Rankine Cycle Specialists Conference sponsored by the
American Institute of Aeronautics and Astronautics
Cleveland, Ohio, October 26-28, 1965

NATIONAL AERONAUTICS AND SPACE ADMINISTRATION

AN EXPERIMENTAL STUDY OF THE CONDENSING CHARACTERISTICS OF MERCURY VAPOR FLOWING IN SINGLE TUBES

by James A. Albers and David Namkoong, Jr.

Lewis Research Center
National Aeronautics and Space Administration
Cleveland, Ohio

E-3244

ABSTRACT

14771

An investigation was conducted to determine the condensing characteristics of mercury vapor flowing in horizontal single tubes. For a crossflow-nitrogen-cooled condenser, flow regime and pressure drop were investigated for nonwetted flow in constant diameter and tapered tubes, under 1 and 0 g, and for wetted flow in tapered tubes under 1 g. For a counterflow-NaK-cooled condenser, heat transfer, inlet pressure, and pressure drop were investigated for a tapered tube under 1 g.

Within the limits of the investigation and predicated on SNAP-8 requirements, the results obtained from the nitrogen-cooled condenser indicated no significant influence of gravity on nonwetted condensing pressure drop. Wetted 1-g condensing frictional pressure drop was higher than that of nonwetted only at the higher flow rates in a tapered tube. Data compared with the Lockhart-Martinelli and fog-flow correlations showed deviation from the former and data scatter on the latter.

Author

For the conditions investigated, the NaK-cooled condenser indicated that the mercury condensing coefficients were higher than the NaK heat-transfer coefficient; therefore the NaK side was the more significant factor affecting the overall heat transfer coefficient. The inlet pressure of mercury, which is intimately related to the mercury inlet temperature and therefore to the heat-transfer mechanism of the condenser, was found to be sensitive to condensing length at shorter condensing lengths and insensitive at the longer condensing lengths.

X-52151

INTRODUCTION

Of the many energy-conversion-system concepts proposed for the generation of electric power for various space flight missions, one of the more promising for the production of higher power levels is the liquid-metal Rankine-cycle turbogenerator system. The development of the SNAP Rankine reactor series characterizes this type of power system. A characteristic of the Rankine cycle system is that the working fluid in the turbogenerator loop undergoes phase changes during the heat-addition and heat-rejection portions of the cycle, resulting in the coexistence of liquid and vapor in continuously varying proportions between the all-liquid and saturated-vapor states. These variable-quality flow conditions represent a major problem in the design of the boiler and condenser components with regard to the prediction of heat-transfer and pressure-drop characteristics. Furthermore, the mixed phase flows are subject to the effects of differing gravity fields to the extent that data on heat transfer and pressure drop obtained in a 1-g environment may not be representative of those to be encountered during system operation in a weightless condition. An additional consideration is the significance of the wettability of the working fluid with regard to types of flow regimes and heat-transfer and pressure-drop characteristics. Finally, the condenser, which is located between the turbine exit and the pump inlet in the system, is restricted to stringent pressure-level and pressure-drop limitations. Because of these considerations, an experimental program was initiated at the NASA Lewis Research Center to determine the condensing characteristics of mercury vapor flowing in single tubes. Values of flow rate and condensing tube geometries were predicated on the SNAP-8 requirements.

This paper describes results obtained from two facilities reflecting two methods of transferring the heat from the mercury vapor condenser. One method simulates heat rejection by radiation, by providing a uniform temperature heat

sink. In this facility, flow regime and pressure drop were investigated for non-wetted flow in constant diameter, and tapered tubes, under 1- and 0-g environments, and for wetted flow in tapered tubes under 1 g. The other method utilizes a liquid metal coolant, NaK, in a counterflow heat exchanger system. In this latter facility, heat transfer, inlet pressure, and pressure drop were investigated in a tapered tube under 1 g. In all cases, the single condensing tubes were oriented horizontally. In addition to obtaining data applicable to the SNAP Rankine cycle, some of the data were analyzed for a more generalized comparison. As such, pressure drop data were compared with the analytical predictions of Koestel et al. and Lockhart-Martinelli in references 1 and 2, respectively.

SYMBOLS

A	Heat transfer area
D_i	Inner tube inside diameter
D_o	Inner tube outside diameter
D_m	Inner tube mean diameter
g_c	Conversion factor
h	Heat transfer coefficient
k	Thermal conductivity
L	Length
LMTD	Log mean temperature difference
l	Distance from condensing tube inlet
l_c	Condensing length
P	Pressure
Q	Heat transfer rate
Δr	Wall thickness
T	Temperature
U	Overall heat transfer coefficient

u	Velocity
x	Quality
μ	Viscosity
ρ	Density
σ	Surface tension
φ_g	Lockhart-Martinelli parameter, $\sqrt{(\Delta P/\Delta L)_{TPF}/(\Delta P/\Delta L)_g}$
χ	Two phase flow modulus, $\sqrt{(\Delta P/\Delta L)_{liq}/(\Delta P/\Delta L)_g}$

Subscripts

g	Mercury vapor
l	Local
liq	Liquid
NaK out	NaK leaving heat exchanger
0	Inlet of condenser
s	Static
TPF	Two-phase frictional
1	One inch from inlet of condenser

APPARATUS FOR CROSSFLOW-NITROGEN-COOLED CONDENSER

A test apparatus was used in which a constant and uniform heat sink was provided along the condensing tube by gaseous nitrogen in crossflow from two manifolds on opposite sides of the tube. Nonwetted data for 1- and 0-g comparison of flow regimes and pressure drop were obtained from the experimental system installed in the bomb bay of a converted Navy bomber (AJ-2). Near zero-gravity durations of about 10 to 15 seconds were obtained by flying the aircraft through a portion of a ballistic path (ref. 3). Data for wetted and nonwetted comparison of pressure drop were also obtained in a ground facility. In both cases, however, the experimental system was essentially the same. In the test system, the heat flux ranged from 30,000 to 92,000 Btu/(hr)(ft^2) depending on the flow

rate and condensing length. Vapor temperature ranged from 800° to 1000° F depending on the vapor pressure and the degree of superheat that was required to minimize liquid carryover. The range of the other variables for the different conditions investigated are listed in table I.

Experimental System

Schematic drawings of a single-pass boiling and condensing system used for 1- and 0-g comparison test are presented in figures 1(a) and (b). The ground facility used for the wetting and nonwetting comparison test is virtually identical to the system shown in figure 1 except that a return line was provided between the receiver and the expulsion unit. In general, the mercury system consisted of an expulsion cylinder, a liquid-flow-measuring unit, a preheater, a high heat flux boiler, a main boiler, a vapor-flow-measuring venturi, a horizontal condensing tube, and a receiver for collecting the condensed mercury.

Definitions of flow characteristics for 1- and 0-g conditions were determined by high-speed photographs of nonwetting condensing in constant-diameter glass tubes of 0.27-, 0.40-, and 0.49-inch inside diameters. Pressure-drop measurements for 1 and 0 g were conducted on both constant diameter and uniformly tapered stainless steel tubes. The constant diameter tube was 87 inches long with an inside diameter of 0.31 inch and a wall thickness of 0.032 inch. The uniformly tapered tube was 84 inches long with an inside diameter of 0.40 inch at the inlet and 0.15 inch at the exit and a wall thickness of 0.025 inch. Pressure-drop measurements for wetted and nonwetted conditions were conducted on 4-feet-long uniformly tapered tubes with an inside diameter of 0.50 inch at the inlet and 0.20 inch at the exit. The nonwetting measurements were conducted with a 0.035-inch-wall stainless steel tube and the wetting measurements with 0.149-inch-wall copper tubes.

Instrumentation

Stainless steel inductance-type pressure transducers, capable of operating in a mercury environment up to 900° F, were used to measure condenser-tube pressure drop, venturi pressures, and venturi pressure drop. In the aircraft, each transducer in direct contact with mercury was mounted with the centerline of the diaphragm parallel to the lateral axis of the aircraft, to minimize the effects of acceleration and deceleration prior to and following the 0-g maneuver. Thermocouples throughout the system were constructed of I.S.A. standard-calibration K Chromel-Alumel wires.

All temperature, pressure, and acceleration data needed for analysis (for the gravity comparison tests) were recorded on two multichannel oscillographs. For the wetted and nonwetted comparison test on the ground, the pressure data were recorded on multichannel oscillographs and the temperatures on self-balancing potentiometer recorders.

Procedure

System operating procedure was identical for both ground and aircraft testing. The mercury loop was initially evacuated to approximately 60 microns of mercury, and the mercury heaters were brought to operating temperature. Startup mercury vapor flow was allowed to purge the system for approximately 5 minutes to remove noncondensables. The receiver pressure was then increased to a constant value (between 14 and 15 psia), and the cooling gas flow was adjusted to establish the mercury interface at the desired location. Relocation of the interface was accomplished by further adjustment of the cooling flow rate.

Determination of the interface location depended on the condensing tube material and the test facility. For the glass-tube tests, the interface was located visually. For the metal tubes in the aircraft (used in 1- and 0-g pressure drop comparison tests), the tube-wall temperatures were scanned to locate

the interface. The interface was identified by the sharp temperature drop in the liquid-mercury leg, which was readily apparent during a rapid scan of the wall temperatures. For the nonwetting and wetting comparison tests, the interface was observed with an X-ray image-intensifier system. The interface for the wetting case was defined as the location where the liquid filled the tube.

The 1- and 0-g comparison tests (of flow regime and pressure drop) were accomplished by recording the 1-g data points in the aircraft while in level flight and 0-g points immediately after without changing system operating conditions. Prior to each data run, a complete calibration of pressure and temperature instrumentation was carried out.

RESULTS FOR CROSSFLOW-NITROGEN-COOLED CONDENSER

Effect of Gravity on Nonwetting Condensing Characteristics

An indication of the differences in flow characteristics in 1- and 0-g environments is shown in figure 2. Under 1-g conditions, droplet runoff down the tube wall was observed, resulting in a liquid accumulation on the bottom of the tube, particularly in the low velocity region. Under 0-g conditions, the drops in the stream and on the wall were more uniformly distributed and had no tendency to "gravitate" toward any part of the tube surface. Whether this apparent difference in flow characteristics is translated into differences of pressure drop is the subject of the following discussion.

The effect of gravity on local static pressure drop is shown in figure 3. The local static pressure drop $(P_0 - P_\ell)_s$ was obtained from the difference between the measured inlet static pressure and the local static pressures along the condensing tube. For both the straight and the tapered tubes, the local static pressure drop increased over the first half of the condensing length due to the high friction losses that resulted primarily from high vapor velocities. In the last half of the condensing tube the pressure rise due to momentum change exceeded the pressure loss due to

friction, resulting in a decrease in local static pressure drop. The data presented for 1- and 0-g conditions were obtained at approximately the same tube inlet flow conditions. With the inlet conditions approximately the same, there was no discernible difference between the distributions of local static pressure drop for 1- and 0-g environments.

The effect of gravity on overall static pressure difference (from inlet to interface) is presented in figure 4. The overall static pressure difference $(P_0 - P_{liq})_s$ was obtained by subtracting the average static pressure in the liquid leg from the inlet static pressure. Examination of the data indicates little difference between the 1- and 0-g conditions, although the majority of the 0-g data fall slightly above the 1-g data. Values of $(P_0 - P_{liq})_s$ ranged from a pressure drop of 0.2 to 2.2 psi for the straight tube and a 0.9-psi pressure rise to a 0.1-psi drop for the tapered tube for the range of condensing lengths and flow rates investigated.

Comparison of Nonwetting Pressure Drop Data with Theory

The experimental pressure-drop data were compared with the two-phase pressure-drop predictions of Lockhart and Martinelli as discussed in reference 2. The two-phase frictional pressure drops between two pressure taps were determined by subtracting the pressure recovery due to the momentum decrease from the measured local static pressure difference. A velocity ratio of one $u_{liq} = u_g$ was assumed in determining the pressure recovery. This assumption is based on the analytical predictions of velocity profiles of liquid drops being entrained into the vapor stream (ref. 1).

Comparison of the nonwetting pressure drop data with the Lockhart-Martinelli correlation (fig. 5) shows that the correlation agrees with the data for the lower values of the parameter X (i.e., corresponding to qualities greater than 0.4). For the higher values of the parameter X (i.e., corresponding to

qualities less than 0.4), the frictional pressure gradient is greater than that predicted by Lockhart-Martinelli, and the deviation increases with an increase in the parameter X. This deviation may result partly from the fact that the flow regimes in dropwise condensing are significantly different from the two-component adiabatic flow model assumed by Lockhart-Martinelli. This deviation may also be because the roughness of the tube wall surface due to the condensed drops on the wall is greater than that obtained by Lockhart-Martinelli, resulting in a larger frictional pressure drop especially for condensation in the low-quality region of the tube.

Though they deviate from the predicted curves, the data points fall into a distinct grouping. Such a grouping suggests a faired data curve through the points such as that shown in figure 5. This curve also fits the faired condensing mercury data points of Koestel et al., as presented in reference 1 as shown in figure 6.

This same set of nonwetting pressure drop data was compared to the fog flow correlation of Koestel et al. (ref. 1). The correlation treats the liquid and vapor as a homogeneous flow and takes into account the buildup of drops on the inside tube wall. As shown in figure 7, the fog flow theory roughly predicts the trend of the nonwetting pressure-drop data over the entire quality range. However, considerable scatter exists.

Effect of Wetting on Pressure Drop

An investigation of pressure drop under wetted conditions, conducted entirely in the ground facility, included photographs of the X-ray image of the interface. The contrast between the interface under wetted and nonwetted conditions is shown in figure 8. Condensation under a nonwetted condition in a tapered tube resulted in a well-defined vertical interface, whereas under a wetted condition an elongated interface that gave rise to periodic waves

resulted. Any difference in pressure drop between wetting and nonwetting flow then may be attributed, at least in part, to the difference in flow regimes as indicated in the figure. Figure 9 indicates that there is no significant difference in the frictional pressure drop for wetted flow compared with the nonwetting condition for the low flow rate (0.028 lb/sec). Greater differences of frictional pressure drop occur in the last half of the condensing length for the mass flow rates of 0.038 and 0.049 pound per second. This may be due to the buildup of the liquid film on the bottom of the tube in wetting condensation, which tended to reduce the vapor-flow area and may have exposed a large area (between the film surface and vapor) of turbulence.

In general, a small, overall static pressure rise was obtained for both wetting and nonwetting conditions at the weight flows and condensing lengths considered as shown in figure 10. At a mass flow rate of 0.028 pound per second, the overall static pressure difference $(P_1 - P_{liq})_s$ was approximately equal for the wetted and nonwetted condensers. At mass flow rates of 0.038 and 0.049 pound per second, values of $(P_1 - P_{liq})_s$ for nonwetted flow exceeded that for wetted flow by 0.3- and 0.6-psi rise, respectively, for the range of condensing lengths considered.

Comparison of Wetting Pressure Drop Data with Theory

A comparison of the wetting pressure-drop data with the Lockhart-Martinelli correlation is presented in figure 11. The result was similar to that found for the nonwetted case in that the data indicated that the experimentally obtained pressure drops were greater than the predicted values at higher X values. Again, a fairly well defined curve could be drawn through the data points. The frictional pressure drops for the wetted condition were slightly greater than those for the nonwetted condition.

The wetting pressure drop data are compared with the fog-flow correlation in figure 12. Under wetting conditions, drops in the vapor stream are formed by the breakup of a thin film that forms on the condensing heat transfer surface. The fog-flow correlation agrees with the wetted data in the high quality region of the condensing tube (i.e., for modified Weber numbers greater than 10). The frictional pressure gradients are higher than predicted, however, for the low-quality region of the condensing tube (i.e., for modified Weber numbers less than 10). This may be due partly to the departure of the wetted flow regime in the low-quality region of the condensing tube from the basis of the fog flow correlation - that of liquid homogeneity within the vapor stream. Again, the data-point scatter is significant.

APPARATUS FOR COUNTERFLOW-NAK-COOLED CONDENSER

Experimental System

A single, tapered, mercury vapor condensing tube, cooled by NaK, was used to obtain heat transfer and pressure data under nonwetted conditions. Tests were conducted entirely in a ground-based facility. A schematic drawing of the mercury-NaK system is shown in figure 13. The range of variables for this experiment is listed in table I. The mercury loop is virtually identical to the nitrogen-cooled mercury vapor condenser system except that a desuperheater was provided between the mercury boiler and the vapor flow measuring venturi. The desuperheater was operated as a heat exchanger such that mercury vapor cooling was accomplished without condensation. By this procedure, high-quality mercury vapor at a saturated condition was provided at the condenser entrance.

The NaK loop is a closed, continuously circulating flow system, consisting of an electromagnetic (EM) pump and an EM flowmeter, an air cooler, and electrical heaters to control the NaK temperature into the heat exchanger. Other branches of the loop provide a means of filling, draining, and filtering the NaK loop.

The condensing tube geometry used was that of a tapered tube, the inner diameter of which was uniformly tapered from a nominal 0.45 inch to 0.20 inch over a length of 40 inches. The inner diameter remained constant at 0.20 inch to the condenser tube exit (12 in.). The annular passage, through which the coolant (NaK) flowed counter to the direction of mercury flow, was maintained at a constant height of 0.10 inch. The condensing tube wall was 0.035 inch, and the tube material was 9M.

Instrumentation

Pressures on the mercury side were measured by stainless steel inductance-type transducers in the high temperature (up to 900° F) sections of the loop and by strain-gage-type transducers for the lower temperatures. Pressure data were recorded on an automatic data-acquisition system and on a continuous trace, galvanometer-type recorder.

Thermocouples throughout the system were constructed of I.S.A. standard-calibration E, Chromel-Constantan wires. On the test section, thermocouples were attached to the outer tube at 1-inch intervals along the tube length; in addition, thermocouples were immersed in the NaK passage at 5-inch intervals. Temperature data used in the analysis were recorded on an automatic data acquisition system.

Procedure

With the NaK lines filled, power was applied to the EM pump to start circulation. The NaK flow rate was indicated by a digital readout from the EM flowmeter.

The procedure for the mercury loop was similar to that of the nitrogen-cooled condenser; that is, the mercury loop was evacuated to approximately 60 microns of mercury, heaters to vaporize mercury were brought up to temperature, and startup mercury vapor was allowed to purge the mercury system to remove

noncondensables. Operating conditions predicated on the SNAP-8 design requirements were reached by gradually increasing mercury flow rate, NaK flow rate, and back pressure, each variable coordinated with the others in a "bootstrapping" operation. With the mercury and NaK flow rates and the NaK inlet temperature at design levels (155 and 515 lb/hr and 500° F, respectively), the interface position was controlled by manipulation of the back pressure.

The interface was located by means of a temperature profile monitor, a visual indication of NaK temperature along the condenser length.

RESULTS OF COUNTERFLOW-NAK-COOLED CONDENSER

Heat Transfer Coefficients

Typical profiles of NaK and mercury temperatures along the condensing length are shown in figure 14. Both the outer-tube (shell) temperatures and the NaK-stream temperatures are shown. These profiles were based on constant values of saturated mercury and NaK flow rates and NaK inlet temperature. While these values were kept constant, the interface was positioned by controlling the condenser back pressure. The NaK temperature profile used in the heat transfer calculations was a curve that was faired through the stream temperature points with the shell data points serving as guides.

The overall heat transfer coefficient was calculated incrementally, for any one NaK-mercury temperature profile, by considering the fluid temperatures entering and leaving any one increment of heat transfer area. This was then plotted as $\int UdA$ on the ordinate and $\int dA$ on the abscissa. Figure 15 is a typical result. Except for a small section of the tube near the inlet, the values are such that a straight line could be drawn through the points. The slope of this line can then be considered as a mean overall heat transfer coefficient for the condenser section. For the range of condensing length considered (7 to 32 in.), the mean overall heat transfer coefficient ranged from 2500 to

3150 Btu/(hr)(ft^2)($^\circ$F). The significance of these values of the overall heat transfer coefficient in determining the mercury condensing coefficient may be seen in figure 16. The range of the mean overall heat-transfer-coefficient experimental values are shown with the mercury condensing coefficient as the ordinate for three values of the NaK heat transfer coefficient. For the conditions covered in this series of tests, the heat transfer coefficient of NaK as calculated from an equation of Dwyer and Tu (ref. 4) was approximately 5000 Btu/(hr)(ft^2)($^\circ$F). The values of 3000 and 8000 Btu/(hr)(ft^2)($^\circ$F) are included as arbitrary curves. The magnitude of the mercury condensation coefficient is indicated by the region of overlap between the expected NaK heat-transfer-coefficient value and the experimental data band. The results indicate that the mercury heat transfer coefficient is greater than 10,000 Btu/(hr)(ft^2)($^\circ$F) and larger than any expected value of the NaK heat transfer coefficient. The NaK heat transfer coefficient then is the more significant factor in affecting the overall heat transfer coefficient.

Inlet Pressure

Determining the characteristic of the mercury inlet pressure as a function of condensing length is important to the designer concerned with turbine performance and pump operation. Where the liquid mercury leg serves as an inventory for the system, the range and limits of condensing length operation must be considered. Finally, the characteristic of the pressure curve affects the type of control that might be considered for condenser pressure or inventory control.

Under saturated conditions, the inlet pressure of the condenser is related to the vapor temperature at the inlet by the pressure-temperature saturation relationship. The inlet temperature, in turn, is dictated by the heat transfer characteristics of the condenser. For a clearer insight into the determination of inlet pressure, then, it is necessary to discuss the factors contributing to

condensing heat transfer.

The basic heat transfer equation with regard to the condenser is:

$$Q = UA(\mathrm{LMTD})$$

Substituting the terms involved in the definition of LMTD and considering the heat transfer area as a function of the condensing length result in

$$Q = \frac{U\, f(\ell_c)\, \Delta T_{NaK}}{\ln\left(1 + \dfrac{T_{NaK}}{T_{Hg} - T_{NaK\ out}}\right)}$$

With further manipulation the equation can be stated in terms of the NaK-mercury temperature difference at the condenser inlet:

$$T_{Hg} - T_{NaK\ out} = \frac{\Delta T_{NaK}}{\left[e^{\exp\left(\frac{U\, f(\ell_c)\Delta T_{NaK}}{Q}\right)} - 1\right]}$$

If the factors on the right hand side are known and $T_{NaK\ out}$ is controlled or determinable, the equation can be solved for T_{Hg}. From the saturation curve the mercury inlet pressure can then be obtained.

In this investigation the mercury and NaK flow rates were constant. The temperature rise of NaK and the overall heat transfer rate, therefore, was constant ($\Delta T_{NaK} = 180^{\circ}$, $Q = 19,400$ Btu/hr) for the range of condensing lengths considered. From the previous discussion on heat transfer coefficients, U ranged from 2500 to 3150 Btu/(hr)(ft^2)($^{\circ}$F). Substituting each of these values and the values of ΔT_{NaK} and Q into the equation results in the curves in figure 17. Each curve then represents an inverse logarithmic function of the NaK-mercury temperature difference with condensing length. On this same set of coordinates, the experimental values of the NaK-mercury temperature difference at the inlet have been plotted. The results indicate a close agreement of the data with the $U = 3150$ Btu/(hr)(ft^2)($^{\circ}$F) curve for condensing lengths less

than 16 inches. The curves tend to converge at the longer condensing lengths.

An additional condition imposed on this system was that of maintaining a constant inlet NaK temperature. This, together with a constant NaK temperature rise, resulted in a constant NaK exit (condenser inlet) temperature. As a consequence, the shape of the NaK-mercury temperature-difference curve is virtually identical to that of the mercury inlet temperature. The mercury inlet pressure determined from the temperature curve, under saturation conditions, together with measured pressure data is shown as a curve in figure 18. The experimental data and the calculated curve, obtained independently, are in good agreement.

The pressure characteristic curve indicates a high sensitivity of the inlet pressure with the shorter condensing lengths. This would be disadvantageous if the condensing length were not controllable in this vicinity. This region would be of advantage, however, if an inventory control system were based on the response to change in the inlet pressure. At longer condensing lengths, the inlet pressure is relatively insensitive; therefore, a change in the condensing length, such as in inventory depletion, will have little effect on the inlet pressure. At the longer condensing lengths, however, pressure drop will increase, a fact which must be considered in the pump operation.

Pressure Drop

The results of the overall static-pressure-drop investigation are shown in figure 19. The data appeared to fall into two distinct groupings, approximately 0.4 psi apart. The discrepancy is still under investigation, but it is felt that the two groupings establish the limits of pressure drop within the set of conditions. In either case there was an overall pressure rise for practically all condensing lengths and a tendency toward a pressure drop was noted for the longer condensing lengths.

SUMMARY OF RESULTS

An experimental study of the condensing characteristics of mercury vapor flowing in horizontal single tubes yielded the following results.

Crossflow-Nitrogen-Cooled Condenser

1. Comparison of 1- and 0-g pressure drop for nonwetter condensing showed no significant difference for all flow rates investigated in constant diameter and tapered tubes.

2. For nonwetted condensing flow, there was an overall static-pressure drop in constant diameter tubes. For wetted and nonwetted flow in tapered tubes, there was an overall static-pressure rise.

3. There was no significant frictional pressure-drop difference between the wetted and nonwetted conditions at the lower flow rates, but there was a greater frictional pressure drop under a wetted condition at the higher flow rates.

4. The Lockhart-Martinelli correlation predicted the experimental values of the frictional pressure gradient accurately in the higher quality region of the condenser; however, the experimental values were higher than the predicted values of Lockhart-Martinelli in the lower-quality region. Though deviating from the predicted curves, the data points fell into a distinct grouping.

5. The experimental data compared with the predictions based on the fog-flow theory showed significant data scatter.

Counterflow-NaK-Cooled Condenser

1. The mean overall heat transfer coefficient, resulting from calculations of local heat transfer data that showed little variation over most of the condensing section, was found to range from 2500 to 3150 Btu/(hr)(ft^2)($^\circ$F) for condensing lengths ranging from 7 to 32 inches.

2. For the conditions investigated, the mercury condensation coefficient was high (above 10,000 Btu/(hr)(ft^2)($^\circ$F) for any expected value of NaK) and constituted a smaller thermal resistance compared with NaK.

3. For the operating conditions investigated, the inlet pressure was determined by the heat transfer characteristics of the condenser, which compared well with the experimental data. This resulted in an inlet-pressure curve that was sensitive to condensing length at the shorter condensing lengths and insensitive at the longer condensing lengths.

4. There was an overall pressure rise for most condensing lengths, with a trend toward a pressure drop at the longer condensing lengths.

TABLE I - RANGE OF VARIABLES FOR MERCURY CONDENSING EXPERIMENTS

Item	Crossflow-Nitrogen cooled					Counterflow-NaK cooled
	Gravity comparison tests			Wetted comparison tests		Nonwetting tests
Gravity level, g's	1 and 0	1 and 0	1 and 0	1	1	1
Wetted condition	Nonwetted	Nonwetted	Nonwetted	Nonwetted	Wetted	Nonwetted
Tube material	Pyrex	304 Stainless steel	316 Stainless steel	304 Stainless steel	Copper	9M
Tube diameter, in.	Constant 0.27, 0.40 0.49	Constant 0.31	Tapered 0.40 to 0.15	Tapered 0.50 to 0.20	Tapered 0.50 to 0.20	Tapered 0.45 to 0.20
Condensing length, in.	68*	45 to 72	45 to 72	18 to 45	18 to 43	7 to 42
Vapor mass flow rate, lb/sec	0.025 to 0.05	0.025 to 0.05	0.025 to 0.05	0.025 to 0.05	0.025 to 0.05	0.041 to 0.045
Vapor inlet quality	0.85 to 1.0	0.85 to 1.0	0.85 to 1.0	0.80 to 1.0	0.80 to 1.0	1.0
Vapor inlet pressure, psia	12 to 26	16 to 22	12 to 22	13 to 18	14 to 19	15 to 22
Vapor inlet velocity, ft/sec	120 to 380	190 to 330	120 to 230	90 to 190	90 to 190	120 to 150
Vapor inlet Reynolds number $\times 10^{-4}$	2.0 to 5.5	3.0 to 5.0	2.0 to 4.0	1.5 to 4.0	1.5 to 4.0	3.0 to 4.0

*Single value

REFERENCES

1. Koestel, Alfred; Gutstein, Martin U.; and Wainwright, Robert T.: Study of Wetting and Nonwetting Mercury Condensing Pressure Drops. NASA TN D-2514, 1964.

2. Lockhart, R. W.; and Martinelli, R. C.: Proposed Correlation of Data for Isothermal Two-Phase, Two-Component Flow in Pipes. Chem. Eng. Prog., vol. 45, no. 1, Jan. 1949, pp. 39-48.

3. Albers, James A.; and Macosko, Robert P.: Experimental Pressure-Drop Investigation of Nonwetting, Condensing Flow of Mercury Vapor in a Constant-Diameter Tube in a 1-G and Zero-Gravity Environment. NASA TN D-2838, 1965.

4. Dwyer, O. E.; and Tu, P. S.: Unilateral Heat Transfer to Liquid Metals Flowing in Annuli. Nucl. Sci. Eng., vol. 15, no. 1, Jan. 1963, pp. 58-68.

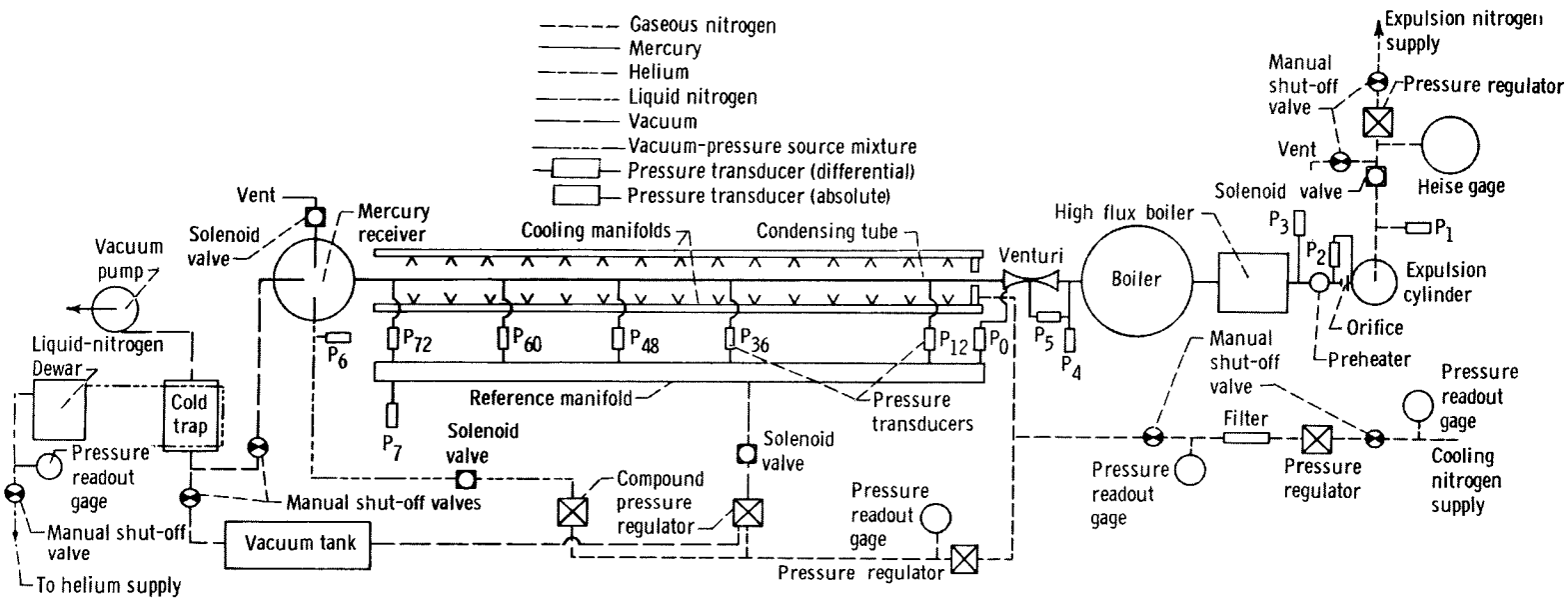

(a) Schematic drawing of system.

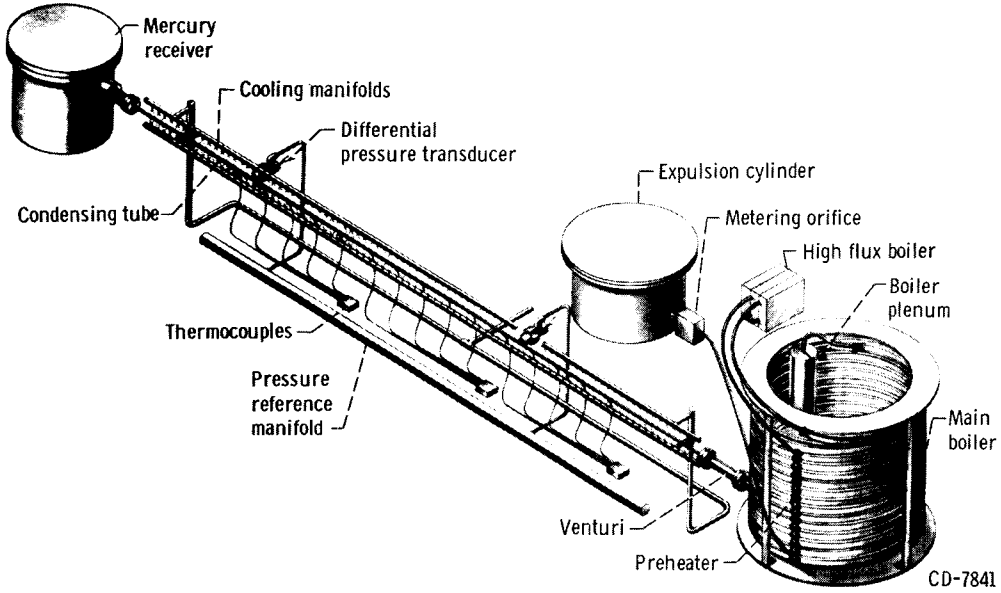

(b) Schematic drawing of components.

Figure 1. - Experimental system and components for crossflow-nitrogen-cooled condenser.

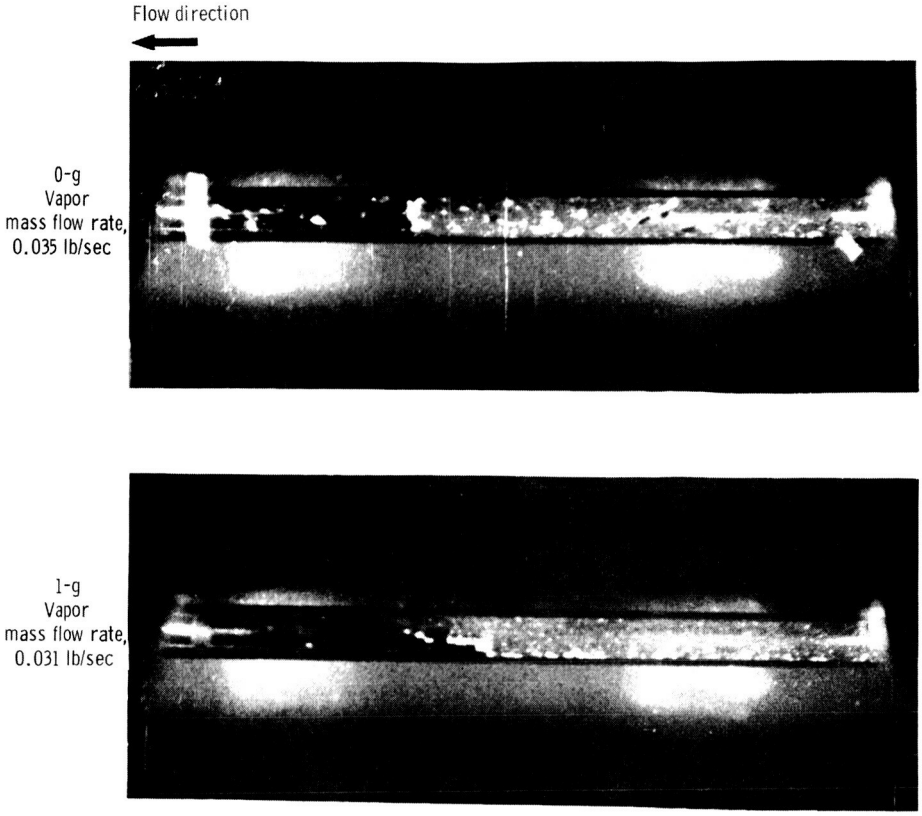

Figure 2. - Flow configurations at interface location for 1- and 0-g mercury nonwetting condensation (3/8-in. o.d. glass tube).

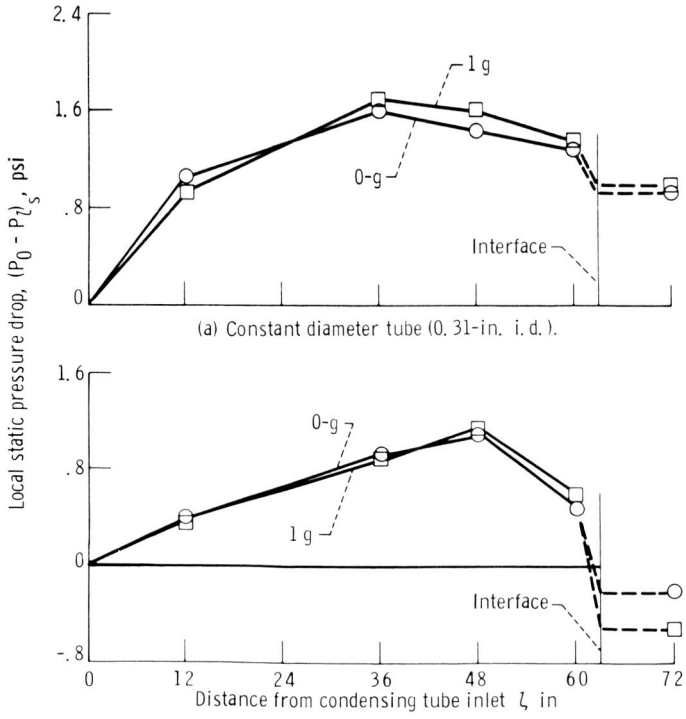

(b) Tapered tube (0.40-in. inlet i.d. with taper ratio, 0.036 in. per ft).

Figure 3. - Effect of gravity on local static pressure drop. (Vapor mass flow rate, 0.038 lb per sec.)

E-3244

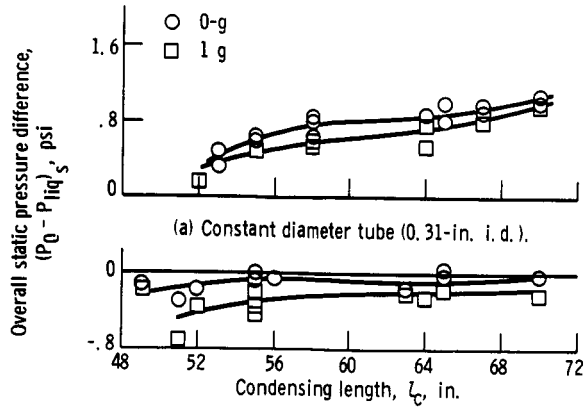

(b) Tapered tube (0.50-in. inlet i.d. with taper ratio, 0.036 in./ft).

Figure 4. - Effect of gravity on overall static pressure difference (vapor mass flow rate, 0.028 lb/sec).

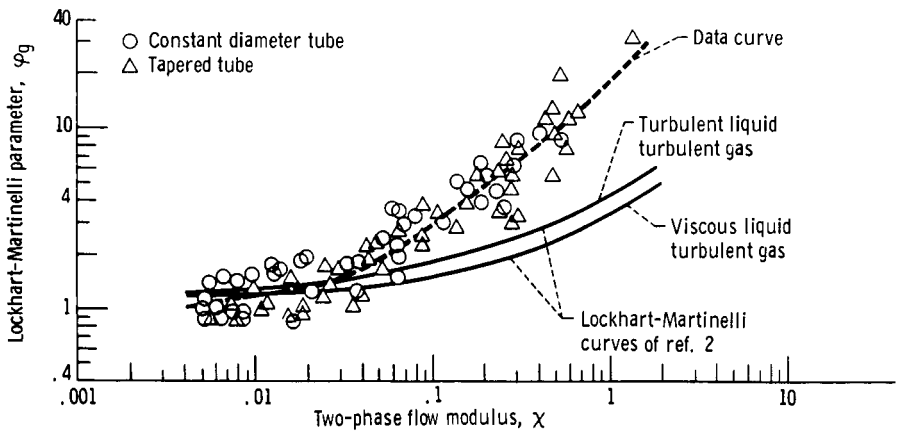

Figure 5. - Comparison of nonwetting data with Lockhart-Martinelli correlation.

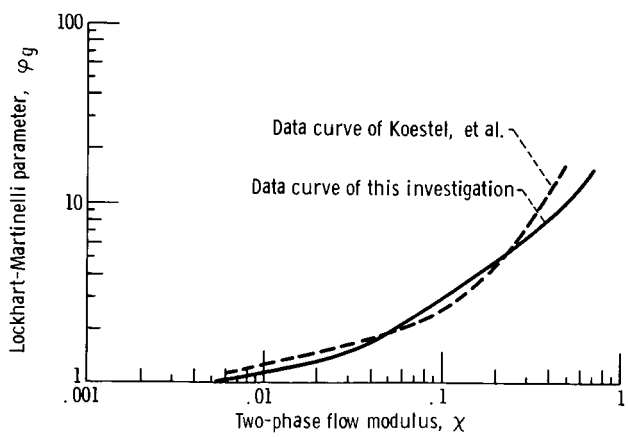

Figure 6. - Comparison of nonwetting data curve of this investigation with the nonwetting data curve of Koestel, et al.

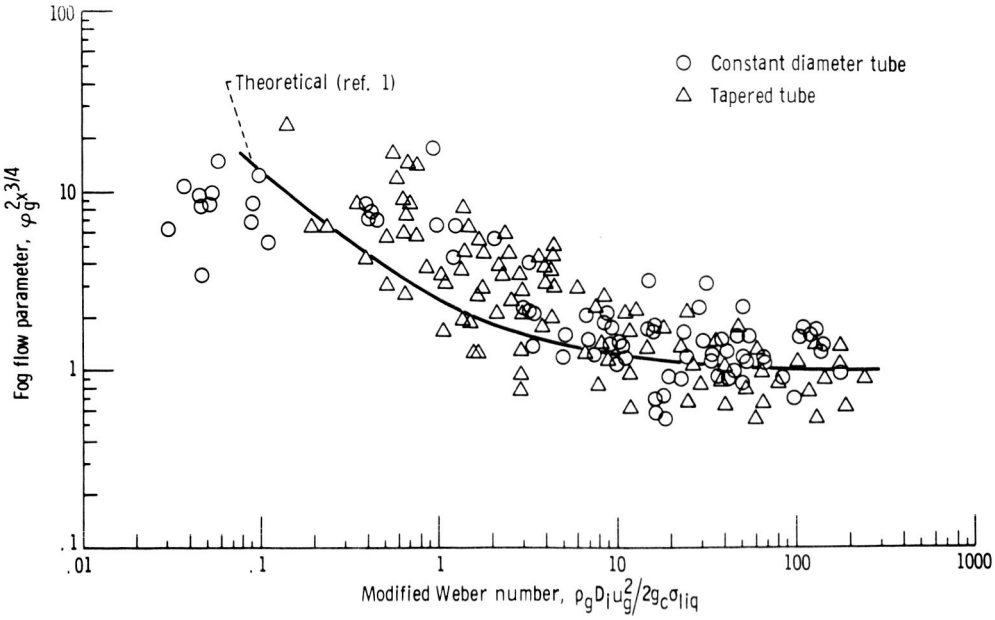

Figure 7. - Comparison of nonwetting data with fog-flow correlation.

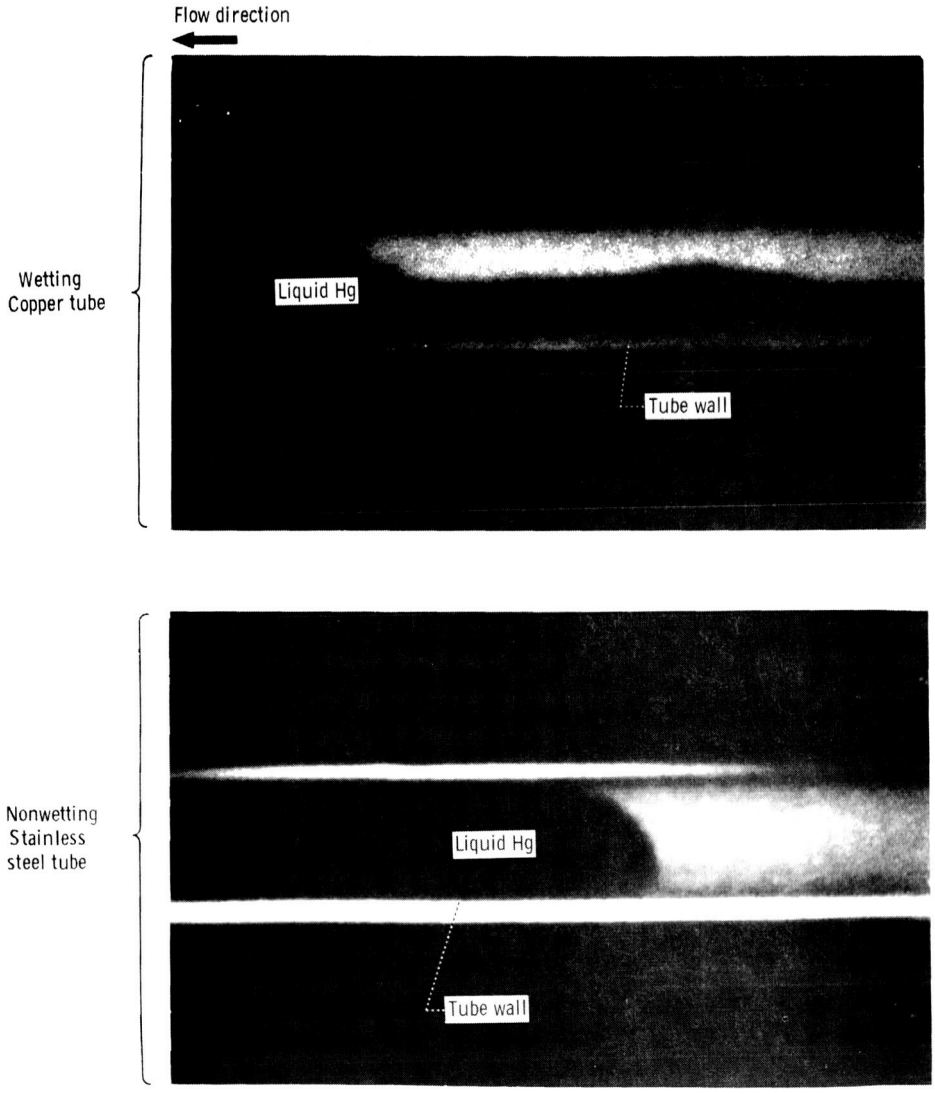

Figure 8. - Flow configurations at interface location for wetting and nonwetting mercury condensation in copper and stainless steel tubes, respectively.

E-3244

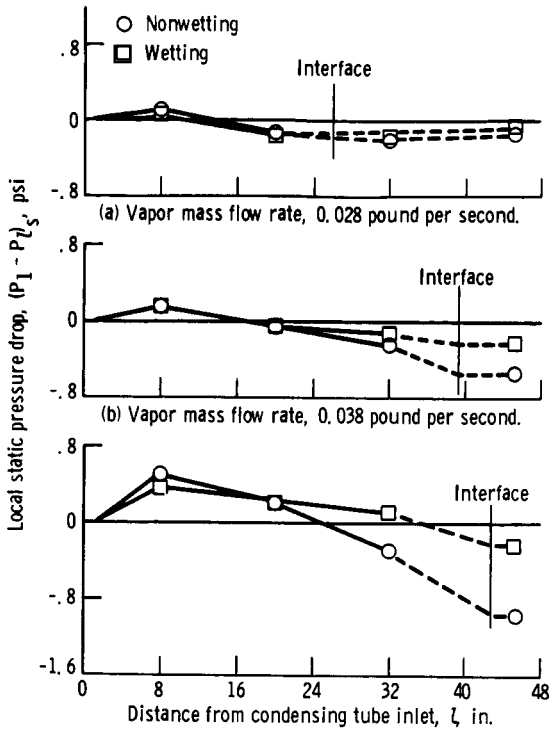

(c) Vapor mass flow rate, 0.049 pound per second.

Figure 9. - Effect of wetting on local static pressure drop (0.50-in. inlet i.d. with taper ratio 0.075 in./ft).

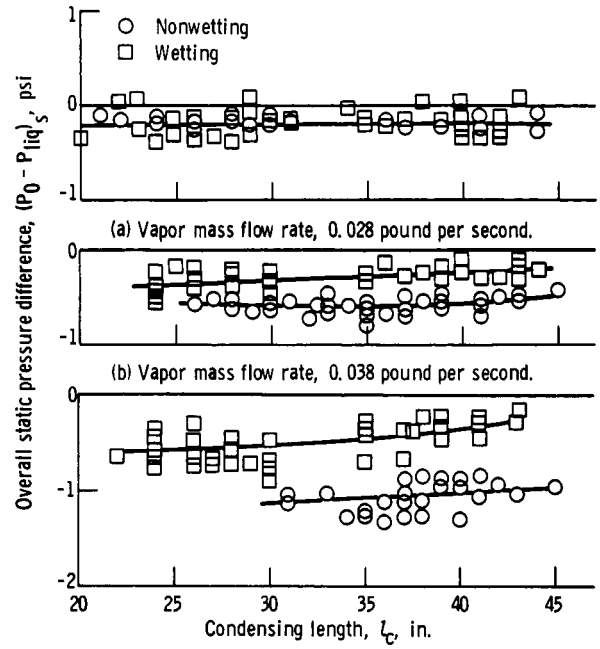

(c) Vapor mass flow rate, 0.049 pound per second.

Figure 10. - Effect of wetting on overall static pressure difference (0.50-in. i.d. with taper ratio 0.075 in./ft).

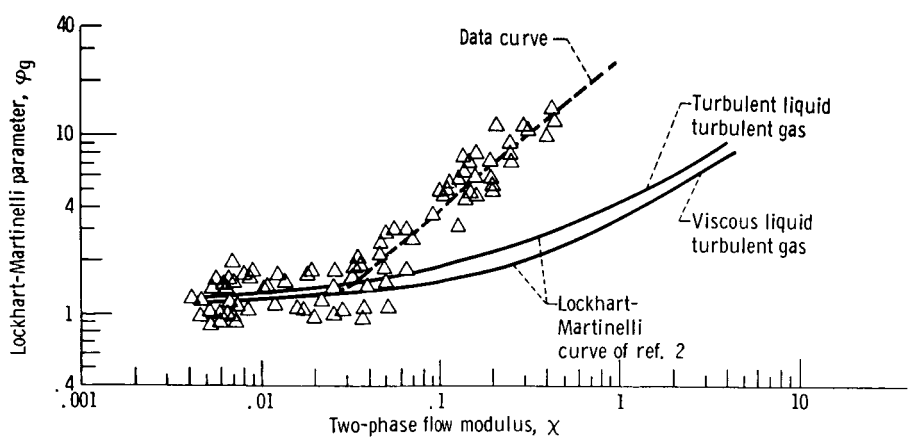

Figure 11. - Comparison of wetting data with Lockhart-Martinelli correlation (tapered tube).

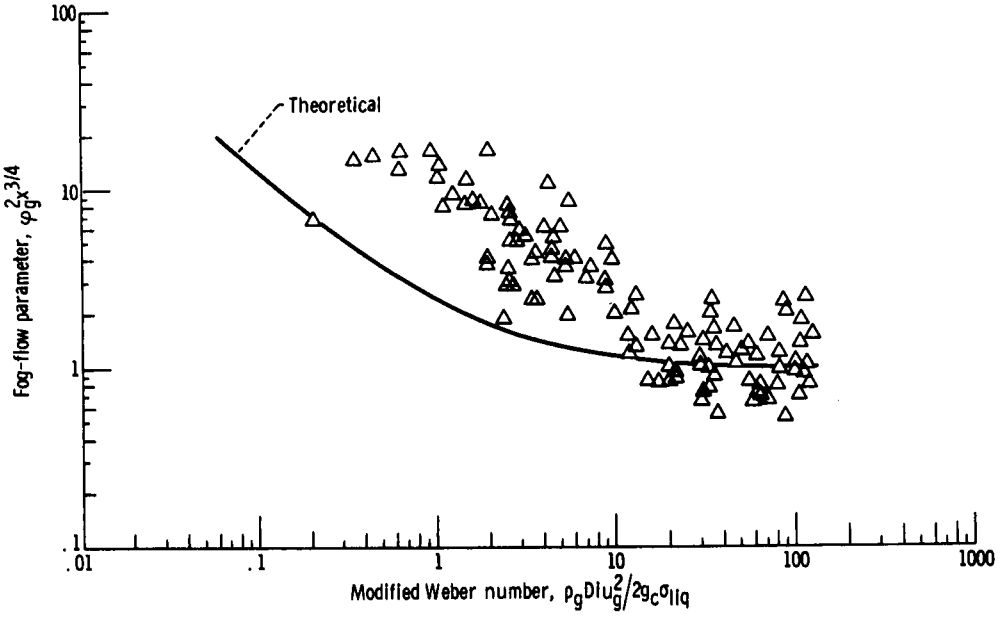

Figure 12. - Comparison of wetting data with fog-flow correlation (tapered tube).

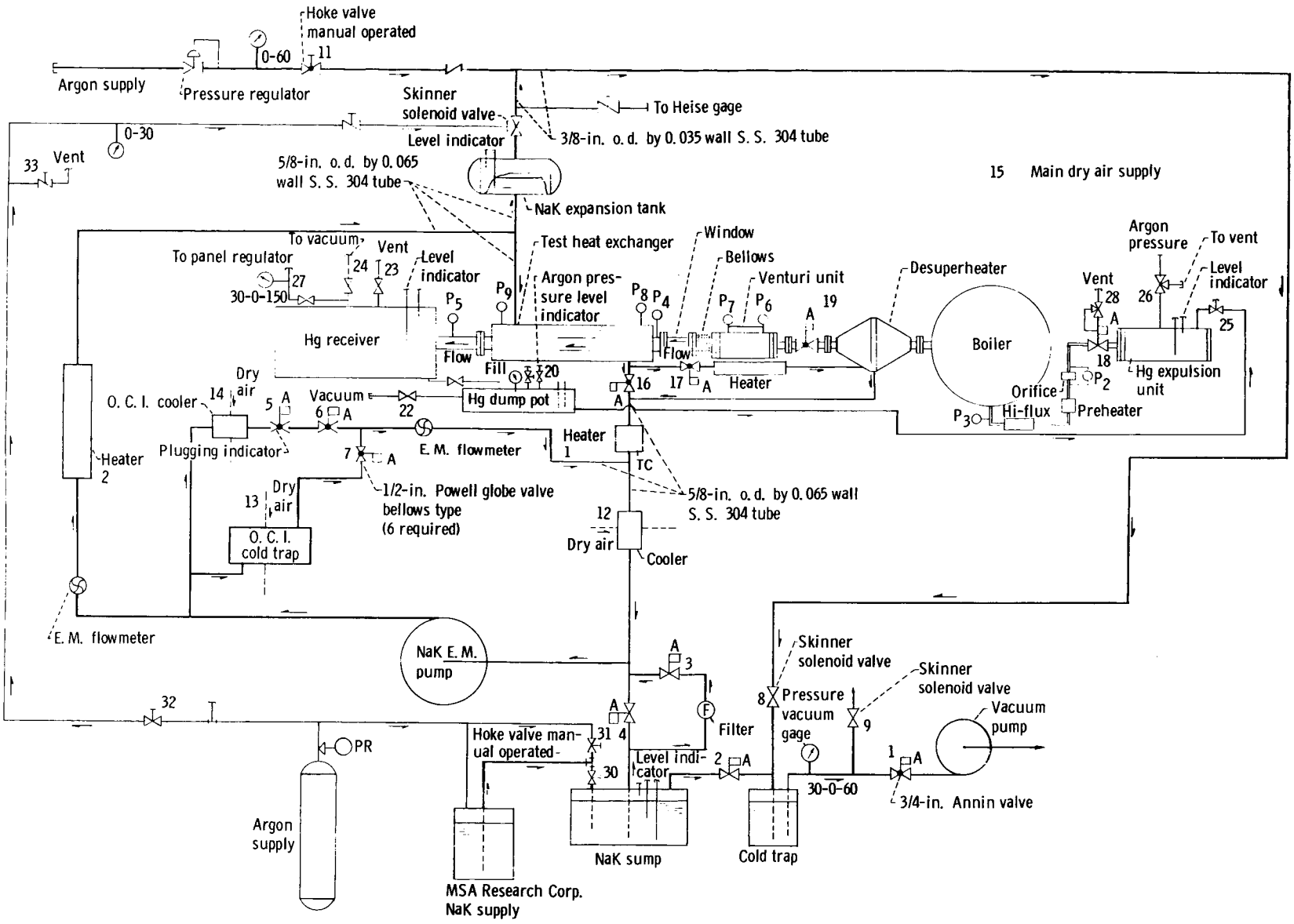

Figure 13. - Experimental system and components for counterflow-NaK-cooled condenser.

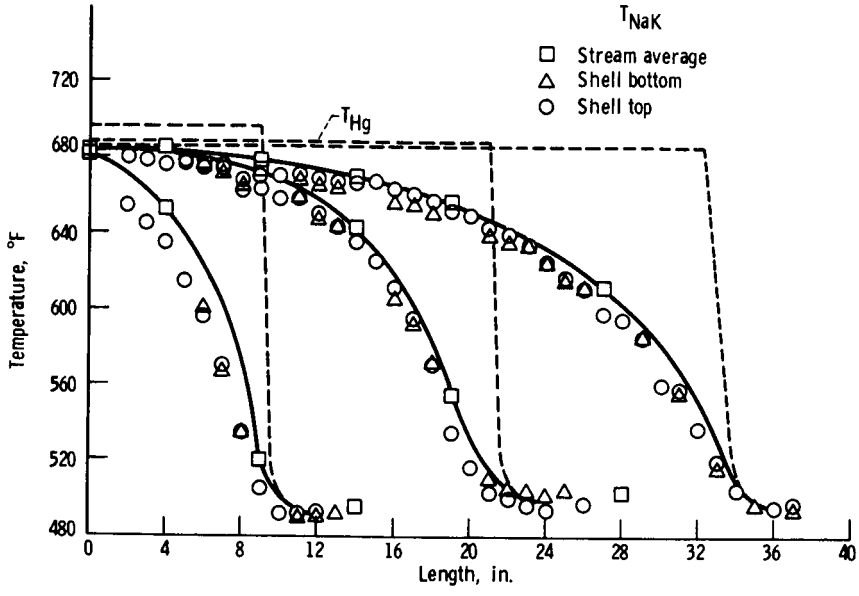

Figure 14. - Temperature distribution of NaK and condensing mercury in counterflow.

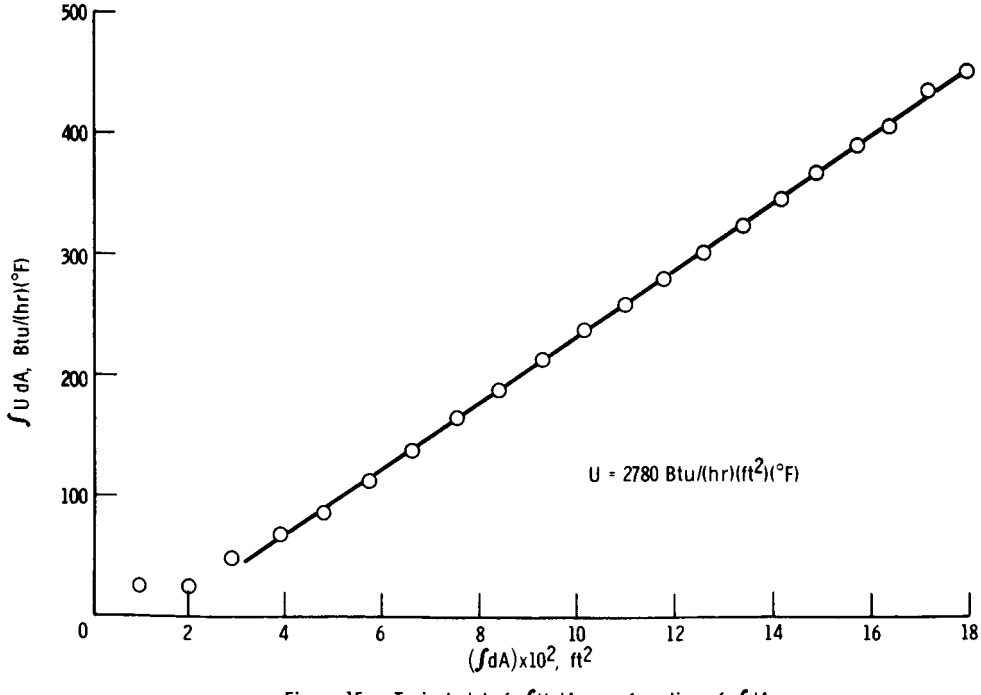

Figure 15. - Typical plot of $\int U\,dA$ as a function of $\int dA$.

E-3244

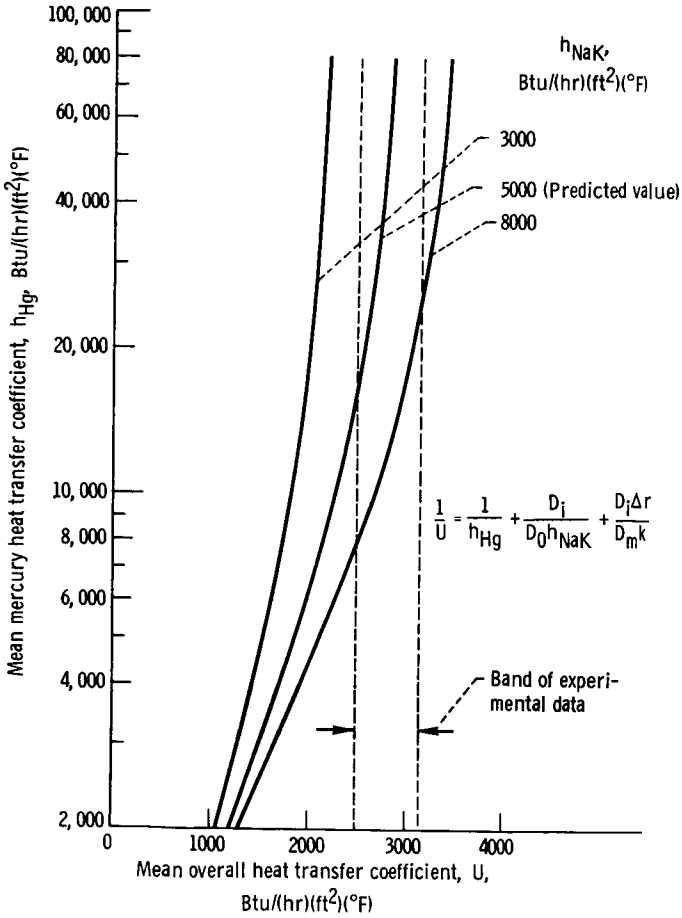

Figure 16. - Mean mercury heat transfer coefficient versus mean overall heat transfer coefficient.

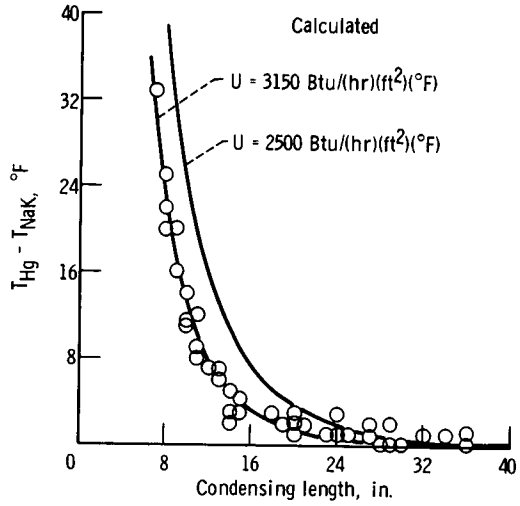

Figure 17. - Condenser inlet temperature difference as a function of condensing length.

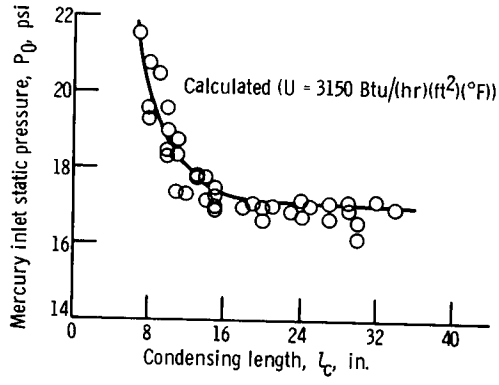

Figure 18. - Mercury inlet static pressure as a function of condensing length for NaK-cooled condenser.

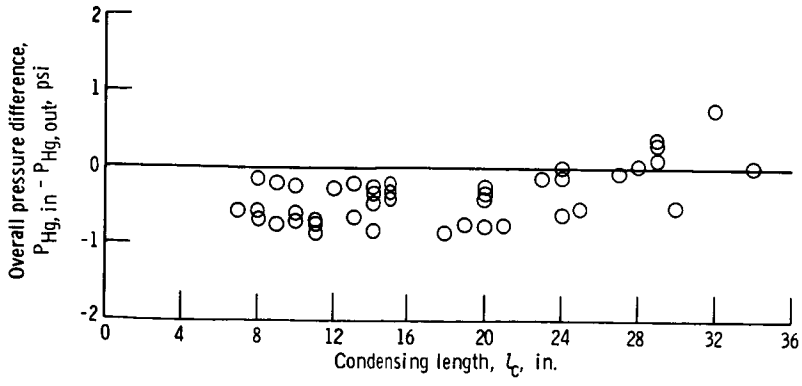

Figure 19. - Overall pressure difference as a function of condensing length.